Δελτίο της Ελληνικής Γεωλογικής Εταιρίας τομ. XXXX, 2007
Πρακτικά 11ου Διεθνούς Συνεδρίου, Αθήνα, Μάιος 2007

Bulletin of the Geological Society of Greece vol. XXXX, 2007
Proceedings of the 11th International Congress, Athens, May, 2007

MORPHOTECTONICS OF THE PSATHOPYRGOS ACTIVE FAULT, WESTERN CORINTH RIFT, CENTRAL GREECE

Tsimi Ch.[1], Ganas A.[1], Soulakellis N.[2], Kairis O.[3], and Valmis S.[3]

[1] *Institute of Geodynamics, National Observatory of Athens, 11810 Athens, Greece*
aganas@gein.noa.gr

[2] *Department of Geography, University of the Aegean, University Hill, 81100 Mytilene, Greece*

[3] *Agricultural University of Athens, Iera Odos 75, 118 55 Athens, Greece*

Abstract

The study area is located on the western part of the Gulf of Corinth which is considered as a paradigm of an active rift system in Greece. This rift was formed by normal slip on big faults which extend the crust of the Earth in the N-S direction. The morphotectonic indices (hypsometric curve, hypsometric integral, drainage basin asymmetry, ratio of valley floor width to valley height) have been estimated using the 20-m digital elevation model of this area and the ARC software. The normal faults of the study area have been extracted by use of a DEM mosaic of 20-m pixel size, satellite images from Landsat 7 ETM+ and SRTM 90m. Our results highlight the recent activity of the Psathopyrgos normal fault on the basis of a series of morphotectonic evidence and suggest the existence of a single fault segment for a distance of 16 km.

Key words: *Morphotectonics, Corinth rift, Psathopyrgos, active faults.*

Περίληψη

Η περιοχή μελέτης είναι στο δυτικό άκρο του Κορινθιακού ανοίγματος. Ο Κορινθιακός κόλπος αποτελεί χαρακτηριστικό παράδειγμα νεοτεκτονικού βυθίσματος στον Ελληνικό χώρο. Το βύθισμα αυτό δημιουργήθηκε από την δράση μεγάλων ρηγμάτων τα οποία ανοίγουν τον φλοιό κατά την διεύθυνση B-N. Με βάση το ψηφιακό υψομετρικό μοντέλο της περιοχή,ς υπολογίστηκαν τέσσερις μορφοτεκτονικοί δείκτες (υψομετρικό ολοκλήρωμα, ασυμμετρία λεκάνης απορροής, λόγος πλάτους κοιλάδας προς ύψος, και ο δείκτης κλίσης). Επίσης χρησιμοποιώντας το ψηφιακό μοντέλο εδάφους, δορυφορικές εικόνες από τον σαρωτή ETM+ του δορυφόρου Landsat 7 και δεδομένα SRTM, έγινε η ψηφιοποίηση των ρηγμάτων της περιοχής μελέτης. Στην συνέχεια, η μελέτη της τεκτονικής γεωμορφολογίας της περιοχής έγινε με χρήση θεματικών χαρτών, οι οποίοι απεικόνιζαν την χωρική κατανομή των δεικτών. Στην εργασία αυτή μελετήθηκε ιδιαίτερα το κανονικό ρήγμα του Ψαθόπυργου το οποίο λειτουργεί ως μία ενιαία, ενεργή δομή μήκους 16 χιλιομέτρων.

Λέξεις κλειδιά: *Μορφοτεκτονική, Κορινθιακό Άνοιγμα, Ψαθόπυργος, ενεργό ρήγμα.*

1. Introduction

The main aim of this work is the understanding of long-term tectonic processes in the Psathopyrgos area of the western Corinth Rift area through the construction of a series of digital maps showing the spatial distribution of the main morphotectonic indices. The morphotectonic analysis helps to identify tectonic processes at the surface (Keller and Pinter, 1996). Our objectives are a) the mapping of the spatial distribution of the morphotectonic indices over a total area of 19.74 square kilometres (km^2, Fig. 1), b) the spatial relationship between the slip rate of the Psathopyrgos active fault and particular indices and c) the creation of a digital database of the geomorphology characteristics in the study region. In this paper we will present a fraction of our results around the Psathopyrgos area that have been validated in the field.

In central Greece, large, shallow earthquakes (M>6) are found to rupture pre-existing fault scarps such as the 1981 earthquakes in the eastern end of the gulf of Corinth (Jackson *et al.* 1982). Every large earthquake creates a permanent deformation at the Earth's surface (Stein *et al.* 1988), resulting in the uplift of the footwall area and the subsidence of the hangingwall area, respectively. The key factor in shaping the landscape in such areas is the relation of the fault slip rate to the erosion rate, in other words in areas deformed by fast-moving faults the geomorphological signal will be much different from areas with slow-moving faults.

The spatial criteria for the recognition of active normal faults are (Jackson and Leeder 1994, Ganas 1997) a) the alignment of fault scarps along the base of mountain fronts b) the elliptical shape of the footwall area as observed in along-fault strike profiles c) the development of axial drainage in the hangingwall area and d) the development of trellis-type drainage in the footwall area with discharge of footwall catchments at both ends of segments. In this work we used a combination of techniques including use of orthorectified Landsat 7 image, a 20-m DEM mosaic and its by-products (slope map, contours, TIN, shaded relief), a 90-m SRTM elevation model, geological data published in the literature and our own field work.

2. The study region

The study area is the western part of the Gulf of Corinth which is considered to be a paradigm of an active rift system in Greece (Fig. 1; De Martini *et al.* 2004, Pavlides *et al.* 2004, Pantosti *et al.* 2004, Bernard *et al.* 2006). This rift was formed by normal slip on large, E-W striking faults which extend the crust of central Greece in the N-S direction. The length of Corinth rift is 130 km and the width is 20-40 km. The major depth is ~900 m and the major height of the mountains around the Gulf of Corinth is ~2500 m. The south coast of the Corinth rift is uplifting whereas the north part is subsiding. From space geodesy we know that the Peloponnesus (southern part) moves faster towards southwest than the Greek mainland (Clarke *et al.* 1998). The result from this movement is that these two areas move away from each other with an average speed of 1 cm/year and increasing from east to west. The bedrock lithology is mainly limestone and the syn-rift rocks are Pliocene - Quaternary age sedimentary rocks such as marls, sandstones, conglomerates and alluvial fan deposits.

In the study region, the active faults have normal kinematics. The area includes some of the most active faults in Greece that have already been studied by many researchers. For example, the Eliki Fault, which is approximately 40 km long ruptured during two important catastrophic earthquakes in 373 BC and in 1861 (Schmidt 1879). Moreover the study area has rugged relief, several major rivers flowing in the general N-S direction (Fig. 1), many narrow valleys and a lot of other interesting landforms. Within our study area the drainage is organized in fifty six (56) catchments. The catchments developed in the footwall area of the Psathopyrgos normal fault amount to fourteen (14). The morphotectonic data for all catchments are presented in Table 1.

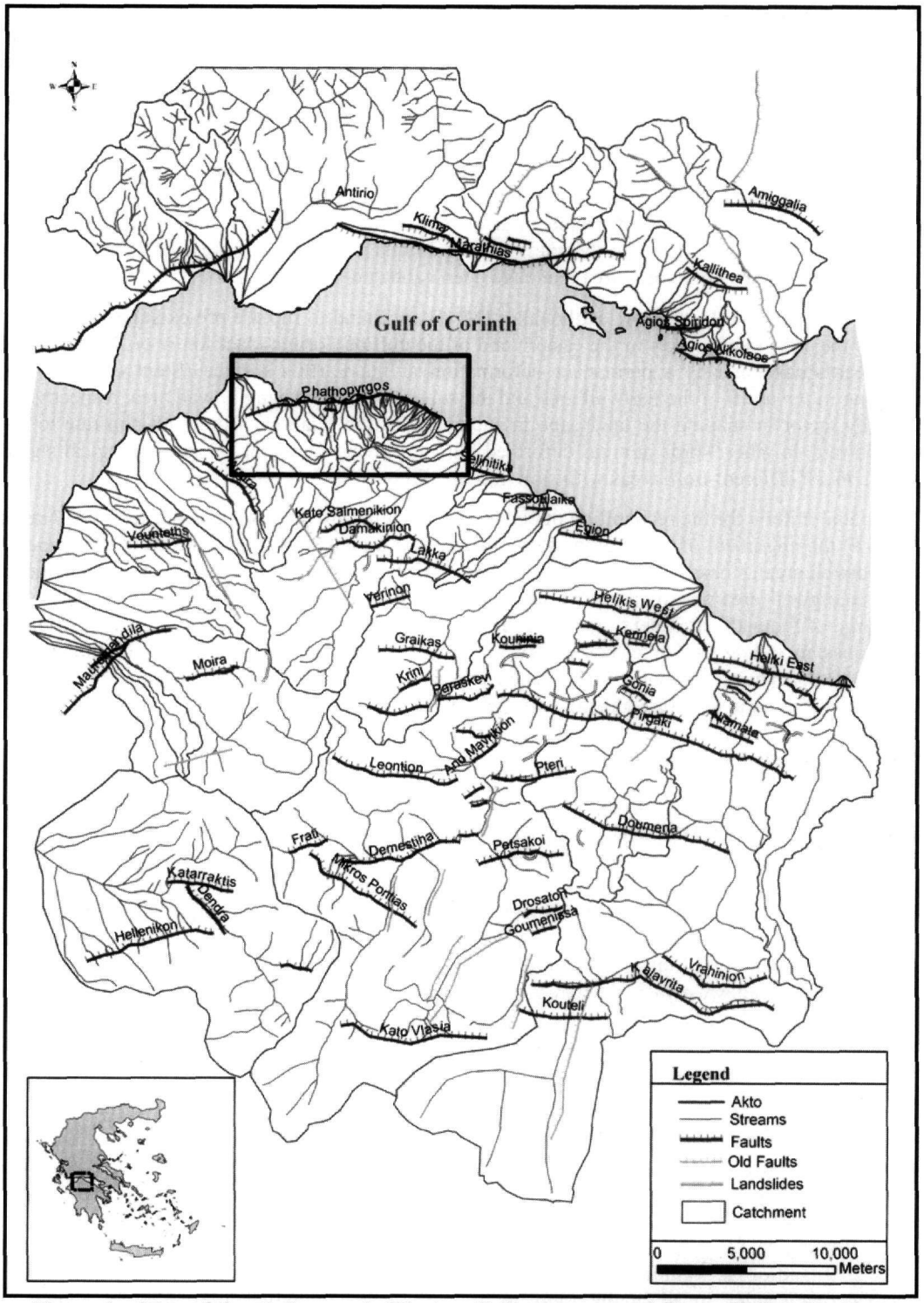

Figure 1 – Map of the study area in Western Peloponnesus and Sterea Hellas. Numbers indicate main catchments. Note the E-W orientation of active faults and the N-S orientation of major rivers. Names of faults are after published literature or by the nearest village/town. Square box indicates the Psathopyrgos fault area

3. Materials and Methods

The software that was used was *ArcGIS™ v.8.1* for Windows. From the available to us digital data, we digitized a) the catchments (56), b) the streams c) the landslides, d) the triangular facets developed on the footwall area of the large, normal faults and e) the normal faults as mapped by Doutsos and Poulimenos (1992), Roberts and Koukouvelas (1996) and by our own field work. The faults were located precisely by collecting fault plane coordinates using field GPS. The feature "active fault" includes 5 fields (attributes) namely the name of the fault, the length, the strike, the distance to the watershed (D to Divide) and the relief of each of them H_{max} - H_{min} (where H_{max} is the maximum elevation in the footwall of the fault and Hmin is the minimum elevation in the hangingwall).

The estimated morphometric indices of this study are the following:

- Hypsometric curve and hypsometric integral *(HI)*

$$HI = \frac{H_{mean} - H_{min}}{H_{max} - H_{min}} \quad (1)$$

where H_{mean}, H_{max} and H_{min} are the mean, maximum and minimum elevation, respectively.

- Drainage basin asymmetry *(AF)*

$$AF = 100 * (Ar/At) \quad (2)$$

where *Ar* is the size of area in the right sub-catchment of main river and *At* is the area of whole catchment.

- Ratio of valley floor width to valley height *(V)*

$$V = \frac{2V_{fw}}{(h_1 - h_3) + (h_2 - h_3)} \quad (3)$$

where V_f is the width of the valley floor, h_1 and h_2 are the elevation of the right and left drainage basic line and h_3 is the elevation of the valley floor.

In this paper we will present the results concerning the spatial distribution of the hypsometric integral (relation 1), the basin asymmetry index (relation 2), and the variation of the slope of the triangular facets along the fault. We also discuss the implications of the above morphotectonic indices and in particular the Valley Height-width ratios (relation 3) for the Psathopyrgos fault.

4. Results and Discussion

Our results are presented in tabular form below (Tables 1, 2) and as maps (Fig. 2 and so on). Table 1 summarises the selected morphotectonic indices for all catchments in Figure 1. Figure 2 presents the spatial distribution of hypsometric integrals and Figure 3 the basin asymmetry, respectively. The map of the hypsometric integral (relation 1) shows very high values in the catchments where their main rivers pour out in the Psathopyrgos and Marathias hangingwall regions (Fig. 2, catchments 13 to 29 and 46 to 50). The Psathopyrgos normal fault strikes E-W and its footwall catchments show values ranging from HI=0.5 to 0.7. The Marathias normal fault also strikes E-W and its footwall catchments range from HI=0.35 – 0.60. This means that these regions have a high mean topography which results from high rates of tectonic activity as demonstrated by the rapid uplift of the footwall of Psathopyrgos fault (0.7-0.8 mm/year; Houghton *et al.* 2003). Also, the hypsometric integral has a relatively high value in the catchments 1 to 5, which have been developed in the footwall area of the Eliki fault. The uplift rate of the footwall area has been determined by De Martini *et al.* (2004) as 1.0- 1.25 mm/year for the East and West Eliki Fault respectively. There is no geological data for uplift rates along the Marathias normal fault.

Table 1- Selected morphotectonic indices of the catchments of the area shown in Figure 1. Shaded rows indicate the catchments of the Psathopyrgos fault

Catchments	Area (m^2)	Af	Vr	Hypsometric Integral	Mean Slope
1	47811930	56.3	0.56	0.48	19.39
2	241417496	43.3	0.29	0.44	19.55
3	84056971	44.7	0.55	0.49	20.96
4	5094981	35.3	0.52	0.39	16.84
5	364478057	53.0	0.34	0.44	18.27
6	64762857	32.2	3.73	0.43	15.45
7	6815984	48.5	1.23	0.31	11.69
8	15683779	27.6	1.38	0.28	13.90
9	2348542	53.7	2.80	0.46	16.59
10	87350558	31.3	4.43	0.40	17.59
11	3121492	44.6	1.21	0.32	10.84
12	1791911	35.3	1.68	0.32	11.05
13	1804260	48.1	1.11	0.49	17.91
14	1359765	48.9	0.43	0.55	17.16
15	699527	38.8	1.15	0.50	18.75
16	1104390	42.6	1.02	0.65	20.17
17	222091	50.7	1.80	0.56	22.27
18	263749	45.7	1.65	0.56	21.86
19	782921	49.2	1.31	0.55	21.20
20	216557	34.0	6.55	0.59	20.64
21	378501	44.7	1.70	0.65	19.85
22	1496489	42.5	1.23	0.61	20.97
23	1632240	58.2	0.41	0.54	26.30
24	3524198	56.7	1.04	0.61	17.46
25	1471935	42.4	1.23	0.65	16.28
26	2623371	60.8	0.66	0.54	19.40
27	3970058	53.6	0.56	0.62	17.79
28	28548291	28.3	0.47	0.35	16.61
29	1033524	23.9	1.04	0.55	18.62
30	2074864	48.2	15.8	0.48	16.25
31	10365813	53.1	1.58	0.42	17.17
32	18112766	58.6	0.64	0.27	13.94
33	21327503	55.9	3.22	0.49	18.07
34	3613023	50.1	-	0.30	8.74
35	13484145	41.8	1.23	0.32	12.18
36	25993049	72.5	1.23	0.27	12.89
37	78844225	67.9	0.61	0.47	16.56
38	11397941	54.7	1.95	0.26	14.12
39	12495250	45.5	0.82	0.57	17.23
40	174732155	-	-	0.29	14.70
41	34297310	40.4	0.90	0.27	15.67
42	876311	46.8	1.38	0.36	17.16
43	1392420	38.3	1.79	0.32	19.13
44	32693871	48.9	3.97	0.45	22.36

45	2901191	47.8	2.22	0.20	6.37
46	143503704	-	-	0.39	19.09
47	31518661	42.1	0.12	0.50	22.17
48	19166567	67.2	0.73	0.55	25.07
49	4367131	42.5	0.67	0.47	21.21
50	13226043	48.1	0.21	0.40	18.41
51	9986878	54.6	1.39	0.40	21.64
52	2878776	35.7	1.26	0.51	22.90
53	1379537	39.2	0.96	0.49	24.33
54	4694924	45.5	0.97	0.46	18.80
55	3191160	41.7	2.23	0.53	20.10
56	71315140	58.5	3.29	0.45	19.67

The map of the Basin Asymmetry factor (AF; relation 2) shows the catchments along the Psathopyrgos fault follow the long-term slip rate distribution, i.e. catchments 14 to 22 show values less than 50 % indicating tilt to the right (east). Catchments 17 and 19 show AF values near 50 indicating the transitional "signal" between the two tilt directions along strike. On the other hand, catchments 23 to 27 show values greater than 50 indicating tilt to the left (west). This result allows us to suggest that Psathopyrgos is a mechanically isolated normal fault, so its footwall profile follows an elliptical shape, therefore tilt direction switches from east to west along strike. Along the Marathias fault the tilt is generally to the west with the exception of catchment 48 (Sergoula stream) which is tilted to the east. Along the Eliki Fault the distal catchments (1 and 5) show values greater than 50 (tilt to the right – east) while the proximal catchments (2, 3 and 4) are tilted to the left (west). As the hinterland of the Eliki fault is also deformed by other, parallel normal faults it is difficult to interpret this tilt pattern. The step over area between the two Eliki segments (Fig. 1) belongs to the catchment of river Kerinitis and shows a moderate tilt to the west (45).

The mean slope map of catchments shows that catchments in the footwall area of Psathopyrgos and Marathias faults have the highest values. Catchment slopes along Psathopyrgos range from 16.2°-26.3° and those along Marathias from 18.4°-25°, respectively. The catchment of Kerinitis river shows the highest mean slope (20.9°) in the footwall area of the Eliki fault.

The Psathopyrgos normal fault at the westernmost end of the Gulf of Corinth (Fig. 1) has been studied in more detail as it shows the characteristic elliptical profile of footwall elevations (Fig. 5). The footwall catchments have been analysed and four morphotectonic indices have been calculated, namely the Hypsometric integral, the mean slope, the valley width-to-height ratio and the basin asymmetry factor. All values are given in Table 3 below.

The footwall area of the Psathopyrgos normal fault is dissected by a dozen of streams with N-S flow. Stream downcutting has developed a series of characteristic erosional landforms along the mountain front, the triangular facets (Fig. 3). Facet slope varies along strike from 15.3° (east end) to 25.8° (west end) with highest values towards the west (slope > 30°; Fig. 4). This data support a weak correlation between mountain front lithology and mean slope of facets. Also, the high mean slope values are characteristic of active faulting (e.g. Ganas *et al.* 2005). A second important observation concerns the east-west distribution of the asymmetry factor (Fig. 6). The catchment asymmetry shows a flip in the tilt direction at about 5 km along strike (from eastward to westward) which is in agreement with the elevation change seen on the footwall profile (Fig. 5). A third observation concerns the distribution of the valley width-to-height ratio. We calculate this ratio upstream of the mountain front for all fourteen catchments along the Psathopyrgos fault (Table 3). The ratio plot (Fig. 6) shows values > 1 at distances 2000-7000 m along strike which is in disagreement with values <1 at both fault ends and towards the middle. This discrepancy is not due to a lack of tectonic uplift and the development of U-shaped valleys in this area but to the

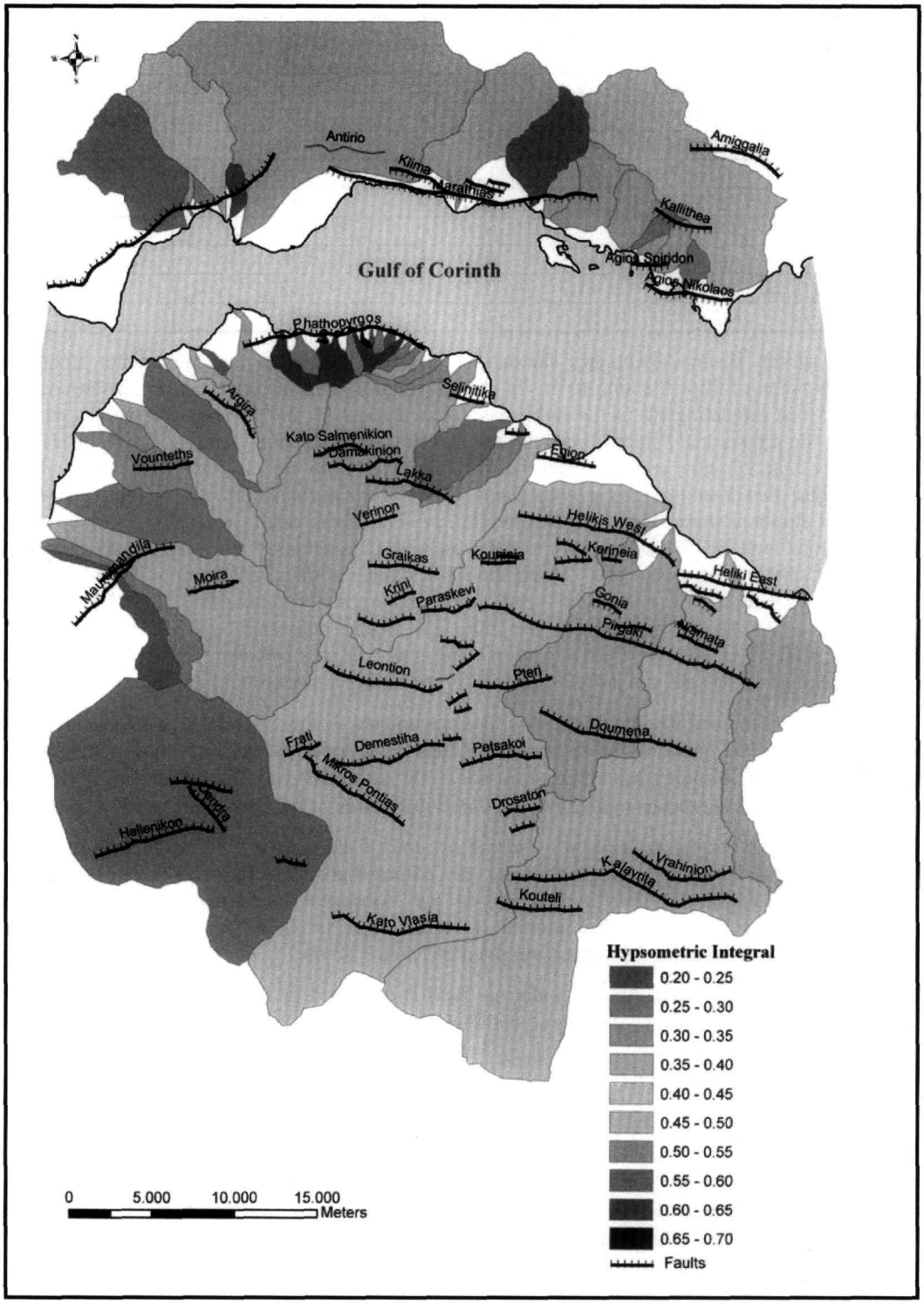

Figure 2 - Map showing the spatial distribution of the hypsometric integral for every catchment. The dark color indicates a high mean topography, while the light color indicates a low topography

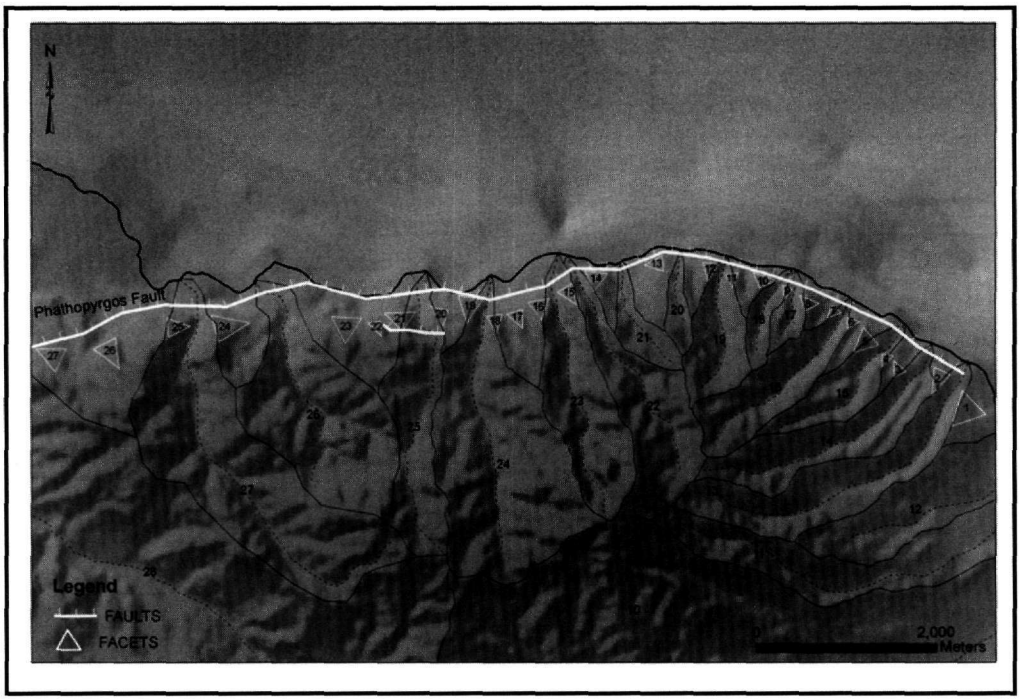

Figure 3 - Map of the Psathopyrgos fault area showing the catchments and triangular facets on its footwall. Integers inside triangles indicate facet numbering along strike

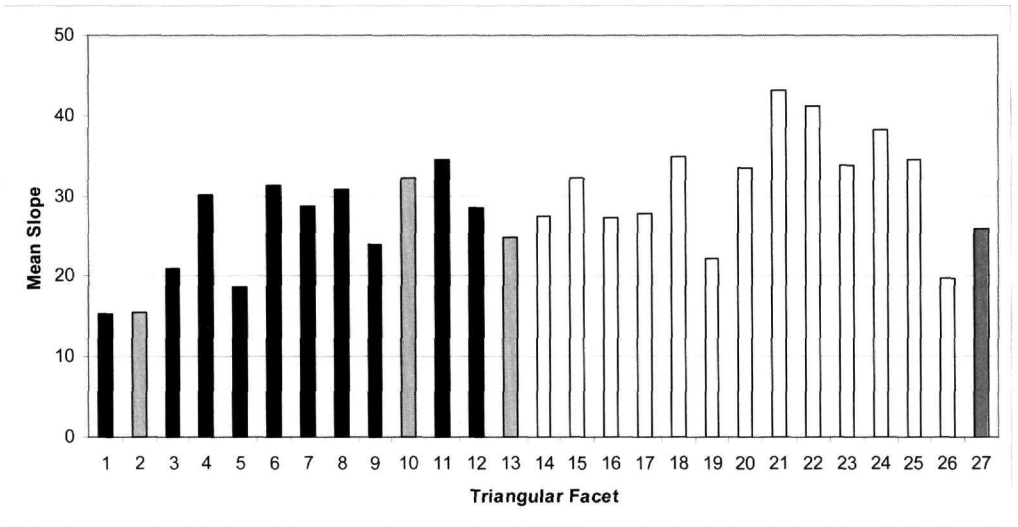

Figure 4 – Bar graph showing the mean slope of the triangular facets along the Psathopyrgos normal fault. Facet colour is according to lithology (Table 2). Facet number is shown in Figure 3

Table 2 – Size (area) and mean slope for each of the triangular facets in the footwall area of the Psathopyrgos Fault. Facet numbering is shown in Figure 3

Number of the Triangular Facets	Area (m^2)	Mean slope (°)	Lithology
1	67500	15.34	Syn-rift (conglomerate)
2	28800	15.45	Syn-rift (scree)
3	12600	20.88	Syn-rift (conglomerate)
4	8100	30.16	Syn-rift (conglomerate)
5	36000	18.71	Syn-rift (conglomerate)
6	8100	31.40	Syn-rift (conglomerate)
7	9000	28.68	Syn-rift (conglomerate)
8	16200	30.85	Syn-rift (conglomerate)
9	8100	24.03	Syn-rift (conglomerate)
10	18000	32.14	Syn-rift (scree)
11	11700	34.48	Syn-rift (conglomerate)
12	19800	28.44	Syn-rift (conglomerate)
13	16200	24.85	Syn-rift (scree)
14	28800	27.44	Pre-rift (limestone)
15	50400	32.22	Pre-rift (limestone)
16	18000	27.28	Pre-rift (limestone)
17	16200	27.89	Pre-rift (limestone)
18	38700	34.84	Pre-rift (limestone)
19	17100	22.17	Pre-rift (limestone)
20	37800	33.53	Pre-rift (limestone)
21	13500	43.16	Pre-rift (limestone)
22	47700	41.18	Pre-rift (limestone)
23	60300	33.77	Pre-rift (limestone)
24	27900	38.18	Pre-rift (limestone)
25	43200	34.44	Pre-rift (limestone)
26	37800	19.76	Pre-rift (limestone)
27	48600	25.87	Syn-rift (marly lim.-scree)

influence of the relatively weak lithology (syn-rift conglomerates). This lithology is more susceptible to hillslope erosion, upstream of the mountain front. Low Vr values (<1) indicate strong incision by streams due to tectonic uplift. For example such values are observed along the Eliki Fault (Verrios *et al.* 2004) where the 1861 earthquake ruptures were observed (Schmidt 1879).

We analysed the elevation profile of the footwall in order to examine if it can be fit by an elliptical line in accordance with other profiles along isolated, normal fault segments in central Greece (Ganas *et al.* 2005). Figure 5 shows the graph showing the footwall elevations along the Psathopyrgos active fault. We observe that the overall elliptical shape is maintained with high confidence as R^2 values range between 0.84 (quadratic fit) and 0.90 (cubic fit).

5. Conclusions

a) We studied the morphotectonics of the western Gulf of Corinth and focused our attention to the Psathopyrgos normal fault. This fault strikes E-W and its footwall catchments show values ranging from HI=0.5 to 0.7. This means that this region has a high mean topography which results from high rates of tectonic activity.

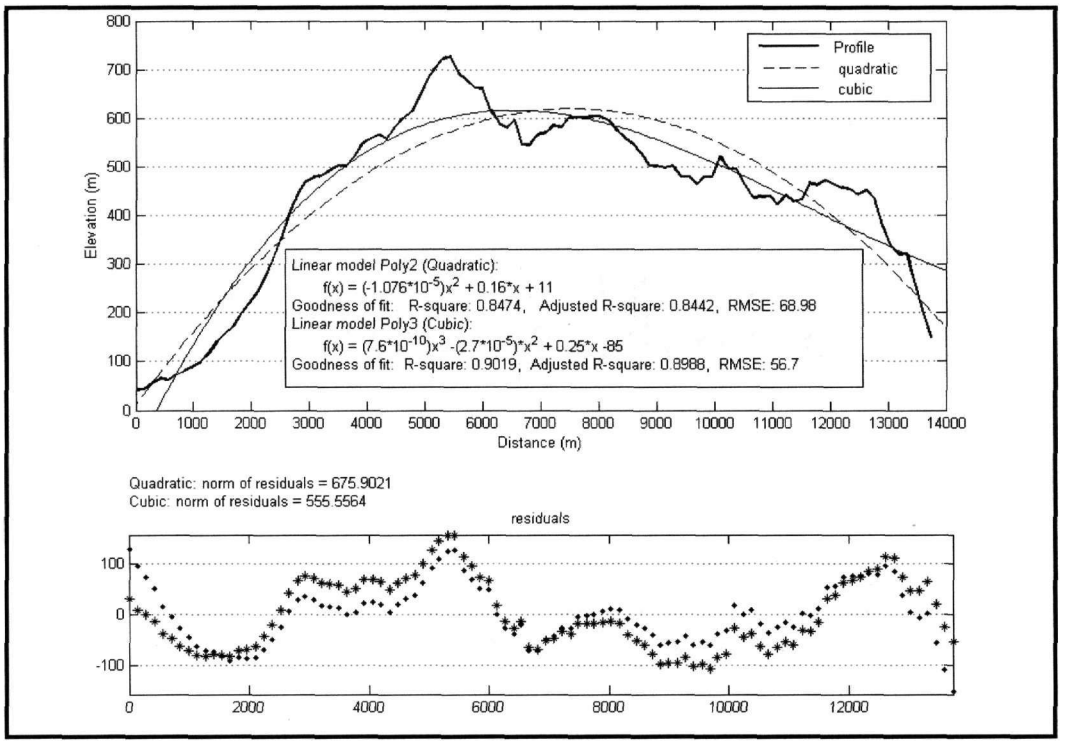

Figure 5 – (Top) Graph showing the footwall elevations along the Psathopyrgos active fault. Also drawn are best-fit curves for quadratic (dashed line) and cubic polynomials (solid line). Vertical exaggeration times 10. (Bottom) Graphs showing goodness of fit along footwall distance. In most cases the cubic fit (dots) is better

Table 3 - Morphotectonic indices along the Psathopyrgos normal fault. The ratio Vr is measured upstream from the mountain front and its distance is given in m

Distance (m)	H. Integral	Mean Slope/rad	Valley (Vr)-Distance to Fault	As/100
468.30	0.55	0.30	0.43 – 1284	0.49
863.29	0.50	0.33	0.98 – 477	0.39
1531.38	0.65	0.35	0.94 – 723	0.43
2148.50	0.56	0.39	1.44 – 282	0.51
2305.50	0.56	0.38	1.20 – 404	0.46
2971.90	0.55	0.37	1.30 – 241	0.49
3474.08	0.59	0.36	1.50 – 464	0.34
4172.08	0.65	0.35	1.40 – 642	0.45
4729.70	0.61	0.37	1.07 – 763	0.43
5018.40	0.54	0.46	0.41 - 623	0.58
5775.60	0.61	0.30	0.97 – 267	0.57
7318.78	0.65	0.28	1.18 – 268	0.42
10611.98	0.54	0.34	0.66 – 689	0.61
14684.12	0.62	0.31	0.56 - 513	0.54

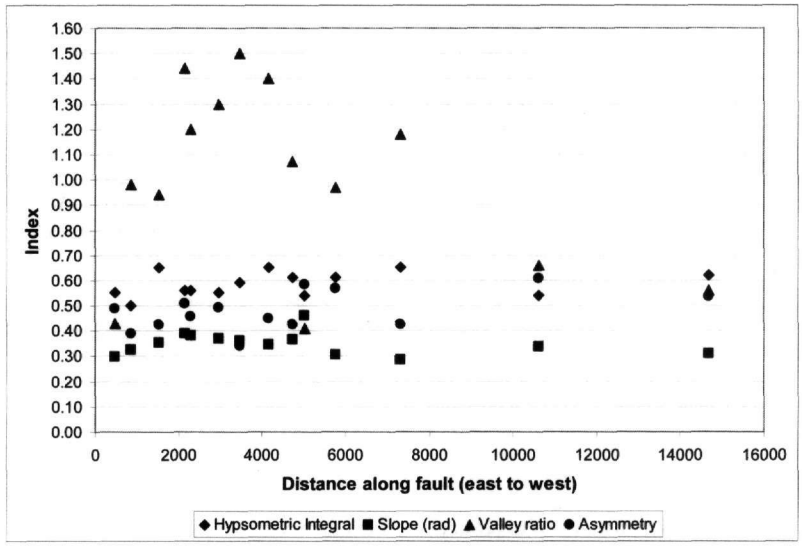

Figure 6 - Graph showing the distribution of morphotectonic indices along the Psathopyrgos Fault. Values of indices are presented in Table 2. In order to maintain a similar Y-axis in this plot the mean slope of catchments is given in radians and the basin asymmetry index is divided by 100

b) The Psathopyrgos fault is a mechanically isolated normal fault, because its footwall elevation profile follows an elliptical shape (Fig. 5) and its footwall tilt direction switches from east to west along strike. The footwall best-fit curve is a cubic polynomial.

c) Mean values of triangular facets are high indicating active faulting. A weak correlation is observed between the mean slope of facets and the lithology of the footwall. Facets developed on limestone have high values (> 30°).

d) The variation of Vr ratio along the Psathopyrgos fault shows values > 1 at distances 2 – 7 km away for the east end. This is not the result of lack of tectonic uplift but it is due to the existence of relatively weak lithology of the syn-rift (conglomerates). Vr values < 1 exhibit valleys developed on bedrock (limestone). In fact, the lowest values of Vr exist at both ends of the fault where long-term slip rates are expected to be the lowest. This observation may suggest that these areas have experienced very recent uplift and intense down-cutting as a result of bi-directional fault growth.

6. Acknowledgments

We thank Professor Pavlides for reviewing the paper and Prof. Hara Drinia for editorial assistance. Sotiris Sboras helped with ARC processing. The 90-m SRTM data set was provided by NASA free of charge. The 20-m DEM mosaic was provided by GEOINFO ltd.

7. References

Bernard, P., Lyon-Caen, H., Briole, P., et al., 2006. Seismicity, deformation and seismic hazard in the western rift of Corinth: New insights from the Corinth Rift Laboratory (CRL), *Tectonophysics,* 426 (1-2), 7-30.

Clarke, P.J., Davies, R.R., England, P.C,. Parsons, B., Billiris, H., Paradissis, D., Veis, G., Cross, P.A., Denys, P.H., Ashkenazi, V., Bingley, R., Kahle, H.-G., Muller, M.-V., and Briole, P., 1998. Crustal strain in central Greece from repeated GPS measurements in the interval 1989-1997, *Geophys. J. Int.,* 135(1), 195-214.

De Martini, P.-M., Pantosti, D., Palyvos, N., Lemeille, F., McNeill, L., and Collier, R., 2004. Slip rates of the Aigion and Eliki faults from uplifted marine terraces, Corinth Gulf, Greece, *C.R.Geoscience,* 336/4-5, 325-334, doi:10.1016/j.crte.2003.12.006.

Doutsos, T., and Poulimenos, G., 1992. Geometry and kinematics of active faults and their seismotectonics significance in the western Corinth - Patras rift (Greece), *Journal. Structural Geology,* 14 (6), 689-699.

Ganas, A., 1997. Fault Segmentation and Seismic Hazard Assessment in the Gulf of Evia Rift, central Greece, *Unpublished PhD thesis,* University of Reading, 369pp.

Ganas, A, Pavlides, S, and Karastathis, V., 2005. DEM-based morphometry of range-front escarpments in Attica, central Greece, and its relation to fault slip rates, *Geomorphology,* 65, 301–319.

Ganas, A., Shanov, S., Drakatos, G., Dobrev, N., Sboras, S., Tsimi, C., Frangov, G., and Pavlides, S., 2005. Active fault segmentation in southwest Bulgaria and Coulomb stress triggering of the 1904 earthquake sequence, *Journal of Geodynamics,* 40(2-3), 316-333.

Houghton, S., Roberts, G., Papanikolaou, I., McArthur, J. and Gilmour, M., 2003. New ^{234}U-^{230}Th coral dates from the western Gulf of Corinth: Implications for extensional tectonics, *Geophysical Research Letters,* 30(19), art. no. 2013.

Jackson, J.A., Gagnepain, J., Houseman, G., King, G.C.P., Papadimitriou, P., Soufleris, C., and Virieux, J. 1982. Seismicity, normal faulting, and the geomorphological development of the Gulf of Corinth (Greece): the Corinth earthquakes of February and March 1981, *Earth planet Sci. Lett.,* 141, 377–397.

Jackson, J.A., and Leeder, M., 1994. Drainage systems and the evolution of normal faults: an example from Pleasant Valley, Nevada. *Journal of Structural Geology*, 16, 1041-1059.

Keller, E., and Printer, N., 1996. *Active Tectonics: Earthquakes, Uplift and Landscape*, Prentice Hall, New Jersey.

Pavlides, S.B., Koukouvelas, I.K., Kokkalas, S., Stamatopoulos, L., Keramydas, D., and Tsodoulos, I., 2004. Late Holocene evolution of the East Eliki fault, Gulf of Corinth (Central Greece), *Quaternary International,* 115-116, 139-154.

Pantosti, D., De Martini, P.M., Koukouvelas, I., Stamatopoulos, L., Palyvos, N., Pucci, S., Lemeille, F., and Pavlides, S., 2004. Palaeoseismological investigations of the Aigion Fault (Gulf of Corinth,Greece), *Comptes Rendus – Geoscience,* 336, 335-342.

Roberts, G. P., and Koukouvelas, I., 1996. Structural and seismological segmentation of the Gulf of Corinth Fault System: implications for models of fault growth, *Annali di Geofisica,* XXXIX, 619-646.

Schmidt, J., 1879. Studien über Erdbeben, *Carl Schottze, Leipzig,* 68–83pp.

Stein, R., King, G.C.P., and Rundle, J., 1988. The growth of geological structures by repeated earthquakes: 2 Field examples of continental dip-slip faults, *Journal of Geophysical Research,* 93(B11),13319-13331.

Verrios, S., Zygouri, V., and Kokkalas, S., 2004. Morhotectonic analysis in the Eliki fault zone (Gulf of Corith, Greece). Bulletin of the Geological Society of Greece, *Proceedings of the 10th International Congress, Thessaloniki, April 2004,* vol. XXXVI, 1706-1715.